Structure and Relative Stability of Drum-like $C_{4n}N_{2n}$ ($n = 3-8$) Cages and Their Hydrogenated Products $C_{4n}H_{4n}N_{2n}$ ($n = 3-8$) Cages

Liang-Wei Shi,[†] Bin Chen,[‡] Jun-Hong Zhou,[‡] Tao Zhang,[‡] Qiang Kang,[‡] and Min-Bo Chen*[,†,‡]

Department of Chemistry, East China University of Science and Technology, 130 Meilong Road, Shanghai 200237, China, and Shanghai Institute of Organic Chemistry, Chinese Academy of Sciences, 354 Fenglin Road, Shanghai 200032, China

Received: February 20, 2008; Revised Manuscript Received: August 29, 2008

The drum-like $C_{4n}N_{2n}$ ($n = 3-8$) cages and corresponding hydrogenated products $C_{4n}H_{4n}N_{2n}$ ($n = 3-8$) are studied at the DFT B3LYP/6-31G** level. Their structures, energies, and vibrational frequencies have been investigated. Comparison of heat of formation reveals that $C_{32}N_{16}$ with D_{8h} symmetry in the $C_{4n}N_{2n}$ ($n = 3-8$) series is a promising candidate as high energy density matter. The calculation of the ΔG and ΔH for the hydrogenation of $C_{4n}N_{2n}$ ($n = 3-8$) shows that it is an exothermic reaction at 298 K and the $C_{4n}H_{4n}N_{2n}$ ($n = 3-8$) species are more stable than $C_{4n}N_{2n}$ ($n = 3-8$) species. The analysis of molecular orbital and selected bond lengths of N−N and C−C provides another insight about their stability. Combined with the nucleus-independent chemical shifts (NICS) calculation, it is indicated that molecular stability for cage-shaped molecules depends on not only aromatic character but also the cage effect.

1. Introduction

During the past 20 years, synthetic and theoretical studies on high energy density matters (HEDM) with pure nitrogen and polymeric nitrogen and their complex with transition metals has been in the mainstream, especially after the N_5^- and N_5^+ molecules were synthesized.[1−4] Those molecules with pure nitrogen and polymeric nitrogen are mainly focused on the N_n formula, in which N_4,[5,6] N_5,[7] N_6,[8] N_7,[9] N_8,[10,11] N_{10},[12] N_{12},[13] N_{18},[14] N_{20},[15,16] and N_{36}[17] species, etc., have been studied theoretically. The complexes of nitrogen with metal have also been discussed computationally.[18−21] There is also some research for nitrogen-rich molecules such as C_xN_y[22,23] and O_xN_y[24,25] species calculated at HF and DFT level. The theoretical exploring with various quantum chemical computation methods makes us believe that some of them might exist in reasonable structures. It is interesting that most of these pure and polynitrogen structures prefer high geometrical symmetry and show cage-like, triangle-like, cycling-like, pentagon-like, drum-like, or helical structures.[26] These intriguing structures and their potential important applications are attracting chemists into this challenging field. The difficulty in this field is in their rare existence in experiments especially for pure nitrogen compounds. To our knowledge, the difficulty at present can hardly be overcome, so one should not be enmeshed into the research of pure nitrogen molecules. People can try to use other atoms such as carbon or boron to partially substitute nitrogen atoms in pure nitrogen structures following the principle of bonding of carbon and nitrogen atoms. Thus, people may pay more expectation to synthesize them.

The idea of the modification on those molecules with polynitrogen and pure nitrogen is aimed to facilitate the work of synthesis under the condition of less loss of main characters as HEDM. An adverse idea can be found from the popular cubane and aza-cubane compounds, in which nitrogen atoms substitute the carbon in the cubane molecule.[27,28] Besides cubane, saturated hydrocarbons with the formula $(CH)_{2n}$ ($n = 3-9$), including the well-known polyhedral hydrocarbons, tetrahedrane, dodecadedrane,[29] and some fullerene cages of $(CH)_n$ (n = 16, 18, 20,[30] 24, 28, 32,[31] 36, 38, 40[32,33]), can undergo the same substitution progress with nitrogen in place of carbon. In fact, heterofullerenes with carbon atoms substituted by heteroatoms, such as boron or nitrogen, have been a focus of attention experimentally and theoretically,[34] since doping can enhance the energy.

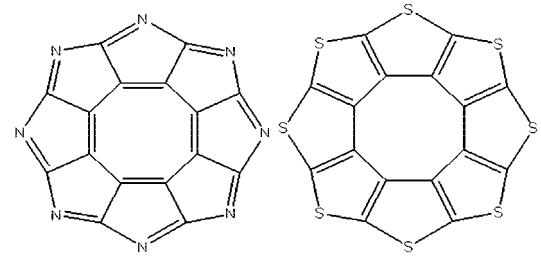

Figure 1. The structures of sunflower-like $C_{16}N_8$ and $C_{16}S_8$ molecules.

Besides the claim of polynitrogen molecules, small caged fullerene, and N-doped fullerenes as HEDM, a sunflower-like new form of carbon−sulfur has recently been synthesized (Figure 1).[35] All of these greatly prompt us to research the analogy. A series of designed molecules $C_{4n}N_{2n}$ ($n = 3-8$) ($C_{12}N_6$, $C_{16}N_8$, $C_{20}N_{10}$, $C_{24}N_{12}$, $C_{28}N_{14}$, $C_{32}N_{16}$) are proposed in this paper, which perhaps would behave in HEDM character if they could be synthesized. These molecules are N-adopted and cage-shaped. Their analogues composed of pure carbon have been studied, and C_{20} to C_{36},[36,37] C_{42}, and C_{48}[38] cages are the representatives. Similar to the hydrogenation of C_{60},[39] the hydrogenated products of our designed $C_{4n}N_{2n}$ ($n = 3-8$) and $C_{4n}H_{4n}N_{2n}$ ($n = 3-8$) ($C_{12}H_{12}N_6$, $C_{16}H_{16}N_8$, $C_{20}H_{20}N_{10}$, $C_{24}H_{24}N_{12}$, $C_{28}H_{28}N_{14}$, $C_{32}H_{32}N_{16}$) are also researched in this paper. All of these newly designed molecules are presented in Figure 2.

Among these designed drum-like molecules, the $C_{32}N_{16}$ molecule is modeled by merging two $C_{16}N_8$ molecules, proposed

* Corresponding author.
[†] East China University of Science and Technology.
[‡] Chinese Academy of Sciences.

10.1021/jp801501g CCC: $40.75
Published on Web 10/24/2008

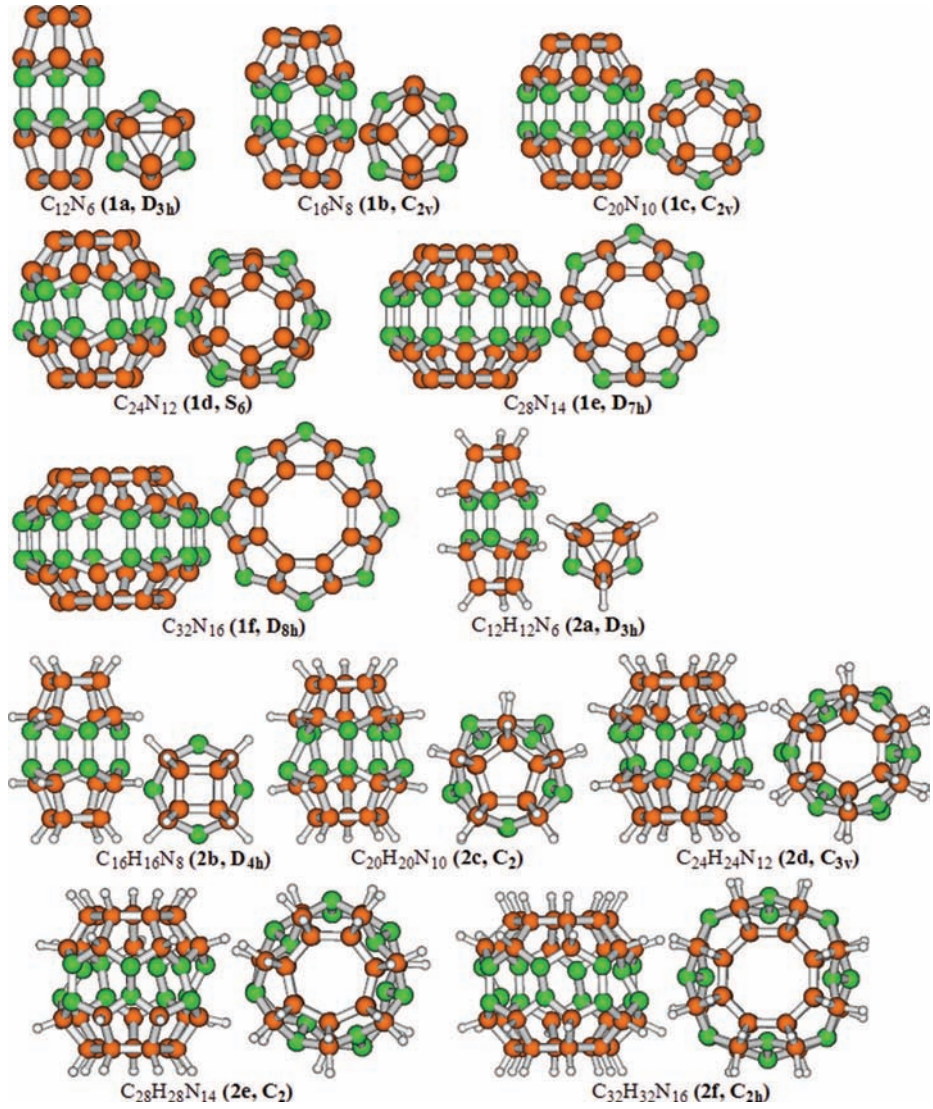

Figure 2. Optimized structures of drum-like $C_{4n}N_{2n}$ ($n = 3-8$) and $C_{4n}H_{4n}N_{2n}$ ($n = 3-8$) cages (side view on the left and plane view on the right). The green color stands for nitrogen atoms, and the orange for carbon.

as an analogue of sunflower-like $C_{16}S_8$ molecule (Figure 1). The $C_{16}N_8$ (ACS: 42210−04−8) is named as 1,12:4,3:7,6:10,9-tetranitrilocycloocta[1,2-*c*:3,4-*c*′:5,6-*c*″:7,8-*c*‴] tetrapyrrole in ACS nomenclature, but no report about its study has been found so far. There are also two analogues, cylindrical N_{18} and phosphorus substitution $N_{12}P_6$, reported recently,[40] similar to the $C_{12}N_6$ and $C_{12}H_{12}N_6$ molecules in shape.

To our knowledge, these designed molecules in Figure 2 have not been reported yet except in a study of an isomer of the **1d** molecule in ref 34. Systematic theoretical studies for the designed species including molecular structures, orbital properties, thermochemical properties, and aromatic character in the present paper might provide heuristic information for future experimental work on HEDM.

2. Computational Details

Full geometric optimization for these 12 drum-like molecules at ground state is performed at B3LYP/6-31G* and B3LYP/6-31G** levels. Actually these two levels are the same for molecules without hydrogen atoms. Usually the geometric optimization for high symmetric compounds is quite difficult. The first step of optimization was performed with the constraint of symmetry in D_{nh}. If imaginary vibrational frequencies exist, the structures with lower symmetry can be further explored. The structure adjustment by the atomic amplitude of the highest/high imaginary frequency is also helpful to the symmetry exploration. The structure after symmetry exploration and atomic position adjustment is then optimized again. One or more imaginary frequencies including the highest one are removed after this round of optimization. This operation might be used several times iteratively with each step of lowering symmetry, until no imaginary frequency exists. So, the structure is thus located at a reasonable minimum on the hypersurface of potential energy. After having established the equilibrium geometries, the electronic stability and orbital energies are investigated. Usually, the vertical ionization potential *I* and the electron affinity *A* can be obtained by Koopman's theorem, which relates them to the negative orbital energies.

The extent of electron delocalization is usually revealed by nucleus-independent chemical shifts (NICS),[41] which equals the negative of the isotropic nuclear magnetic shielding tensor of the ghost atom. It has also been used to indicate the aromatic character for some polyhedral hydrocarbon and doped fullerenes.[34] In the next section, the gauge-independent atomic orbital (GIAO) method was used in the calculation of NICS at the B3LYP/6-31G** level for studying the molecular aromatic

TABLE 1: Total Energies ϵ_0 (au), $\Delta H°_f$(kcal/mol), Group ϵ_0 (au), and Group $\Delta H°_{f,298K}$ (kcal/mol) of 1a−f and 2a−f Series and the ΔG (kcal/mol) and ΔH (kcal/mol) of Hydrogenation Reaction of 1a−f Series

							hydrogenation reaction of **1a−f**		
species	formulas	ground state ϵ_0	$\Delta H°_f$	group ϵ_0	group $\Delta H°_f$	S(298K) [a]/cal·mol^{-1}·K^{-1}	reaction	ΔG[b]	ΔH
1a	$C_{12}N_6$	−784.75279	778.77	−261.58426	259.59	88.757	**1a** + $6H_2$ → **2a**	−499.88	−556.39
1b	$C_{16}N_8$	−1046.61741	874.94	−261.65435	218.74	99.426	**1b** + $8H_2$ → **2b**	−537.34	−613.01
1c	$C_{20}N_{10}$	−1308.58836	902.89	−261.71767	180.58	115.857	**1c** + $10H_2$ → **2c**	−498.45	−593.54
1d	$C_{24}N_{12}$	−1570.52734	954.92	−261.75456	159.15	114.795	**1d** + $12H_2$ → **2d**	−455.67	−566.04
1e	$C_{28}N_{14}$	−1832.45833	1005.16	−261.77976	143.59	131.013	**1e** + $14H_2$ → **2e**	−367.46	−497.54
1f	$C_{32}N_{16}$	−2094.38076	1062.20	−261.79760	132.78	133.440	**1f** + $16H_2$ → **2f**	−268.41	−414.01
2a	$C_{12}H_{12}N_6$	−792.77295	222.38	−264.25765	74.13	86.034			
2b	$C_{16}H_{16}N_8$	−1057.09458	261.93	−264.27365	65.48	94.686			
2c	$C_{20}H_{20}N_{10}$	−1321.40104	309.35	−264.28021	61.87	108.247			
2d	$C_{24}H_{24}N_{12}$	−1585.65717	388.88	−264.27620	64.81	118.192			
2e	$C_{28}H_{28}N_{14}$	−1849.84946	507.62	−264.26421	72.52	130.601			
2f	$C_{32}H_{32}N_{16}$	−2114.00961	648.19	−264.25120	81.02	143.208			
	H_2					31.133			

[a] Entropy was calculated upon the principle of statistical thermodynamics in Gaussian03. [b] ΔG was calculated by $\Delta G = \Delta H - T\Delta S$.

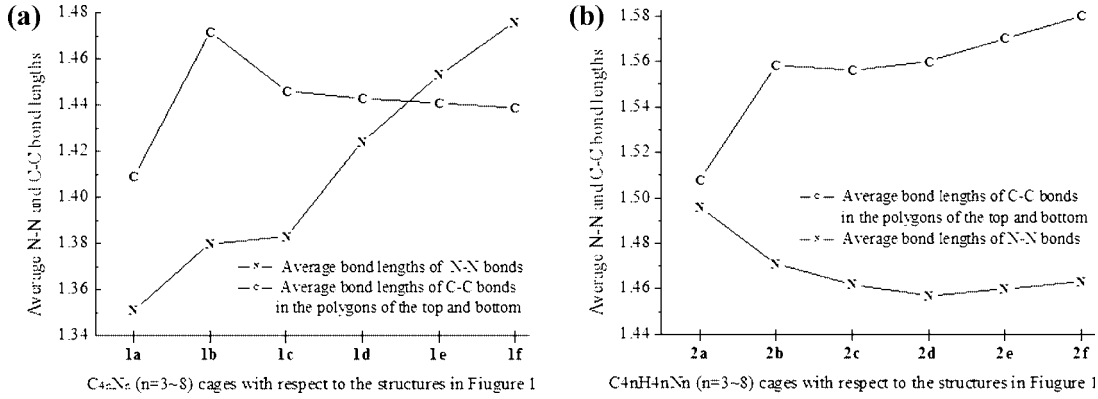

Figure 3. Average N−N bond lengths and C−C bond lengths in the cycles of the top and bottom polygons. (a) for $C_{4n}N_{2n}$ (n = 3−8) and (b) for $C_{4n}H_{4n}N_{2n}$ (n = 3−8).

character. Due to the position dependence of NICS, three representative points were taken for our NICS calculation, namely the point in the geometric center of the molecule and those of the geometric centers in the top and bottom polygons were taken for the target molecules under research. All of the calculations are performed with the Gaussian 03 program.

3. Results and Discussion

3.1. Geometries. The initial optimizations for $C_{12}N_6$, $C_{28}N_{14}$, $C_{32}N_{16}$, $C_{12}H_{12}N_6$, and $C_{16}H_{16}N_8$ were successful without imaginary frequency, and ended up with D_{3h}, D_{7h}, D_{8h}, D_{3h}, and D_{4h} symmetry, respectively. The initial optimizations for $C_{16}N_8$ (D_{4h}), $C_{20}N_{10}$ (D_{5h}), $C_{24}N_{12}$ (D_{6h}), $C_{20}H_{20}N_{10}$ (D_{5h}), $C_{24}H_{24}N_{12}$ (D_{6h}), $C_{28}H_{28}N_{14}$ (D_{7h}), and $C_{32}H_{32}N_{16}$ (D_{8h}) ended up with highest imaginary frequency at i2043, i219, i379, i164, i383, i462, and i459 cm^{-1}, respectively. Their optimization was finished by symmetry exploration and atomic position adjustment, and gave final symmetry of C_{2v}, C_{2v}, S_6, C_2, C_{3v}, C_2, and C_{2h}, respectively.

All of these optimized structures are depicted with side view and plane view in Figure 2. They look like a drum. Due to the difficulty in naming these molecules, we call them drum-like **1a**, **1b**, **1c**, **1d**, **1e**, and **1f** for $C_{4n}N_{2n}$ (n = 3−8) and hydrogenated drum-like **2a**, **2b**, **2c**, **2d**, **2e**, and **2f** for $C_{4n}H_{4n}N_{2n}$ (n = 3−8). All the structures in Figure 2 are comprised of 2n (n = 3−8) five-membered rings and n (n = 3−8) six-membered rings except the top and bottom polygons. The selected geometric parameters (in Å for bond lengths and degree for angles) of the $C_{4n}N_{2n}$ (n = 3−8) and $C_{4n}H_{4n}N_{2n}$ (n = 3−8) species are provided in Supporting Information S1.

The cage effect is more or less an obscure concept. However, for the model compounds of this paper, it is evident from Figure 3 that all the bond lengths in $C_{4n}N_{2n}$ (n = 3−8) are less than those in general in $C_{4n}H_{4n}N_{2n}$ (n = 3−8). The $C_{4n}N_{2n}$ (n = 3−8) series exhibits a condensed structure due to the conjugation and cage effects, while the $C_{4n}H_{4n}N_{2n}$ (n = 3−8) series behaves quite normally.

For the $C_{4n}N_{2n}$ (n = 3−8) series, the average C−C bond lengths in the top and bottom polygons are 1.472 Å for **1b**, 1.446 Å for **1c**, 1.443 Å for **1d**, 1.441 Å for **1e**, and 1.439 Å for **1f**. The average N−N bond lengths are 1.380 Å for **1b**, 1.383 Å for **1c**, 1.424 Å for **1d**, 1.453 Å for **1e**, and 1.476 Å for **1f**. Apparently, the N−N bond length in **1f** is close to that in NH_2−NH_2, 1.489 Å calculated at the B3LYP/6-31G** level, which indicates normal stability for N−N bonds in **1f**. The Π conjugation or delocalization effect within the top or bottom "semisphere" strengthens the bonding among the atoms in the "semisphere", and simultaneously reduces the bonding between the "semispheres". As the cage becomes bigger, e.g. from **1b** to **1f**, the bonds within the region of delocalization, where the C−C bonds in the top and bottom polygons are located, are strengthened or shortened, and the bonds between the two regions of delocalization, i.e. N−N bonds, are reduced or elongated.

To explain the curve of the calculated value of C−C bond lengths on the top or bottom polygon in $C_{4n}H_{4n}N_{2n}$ (n = 3−8)

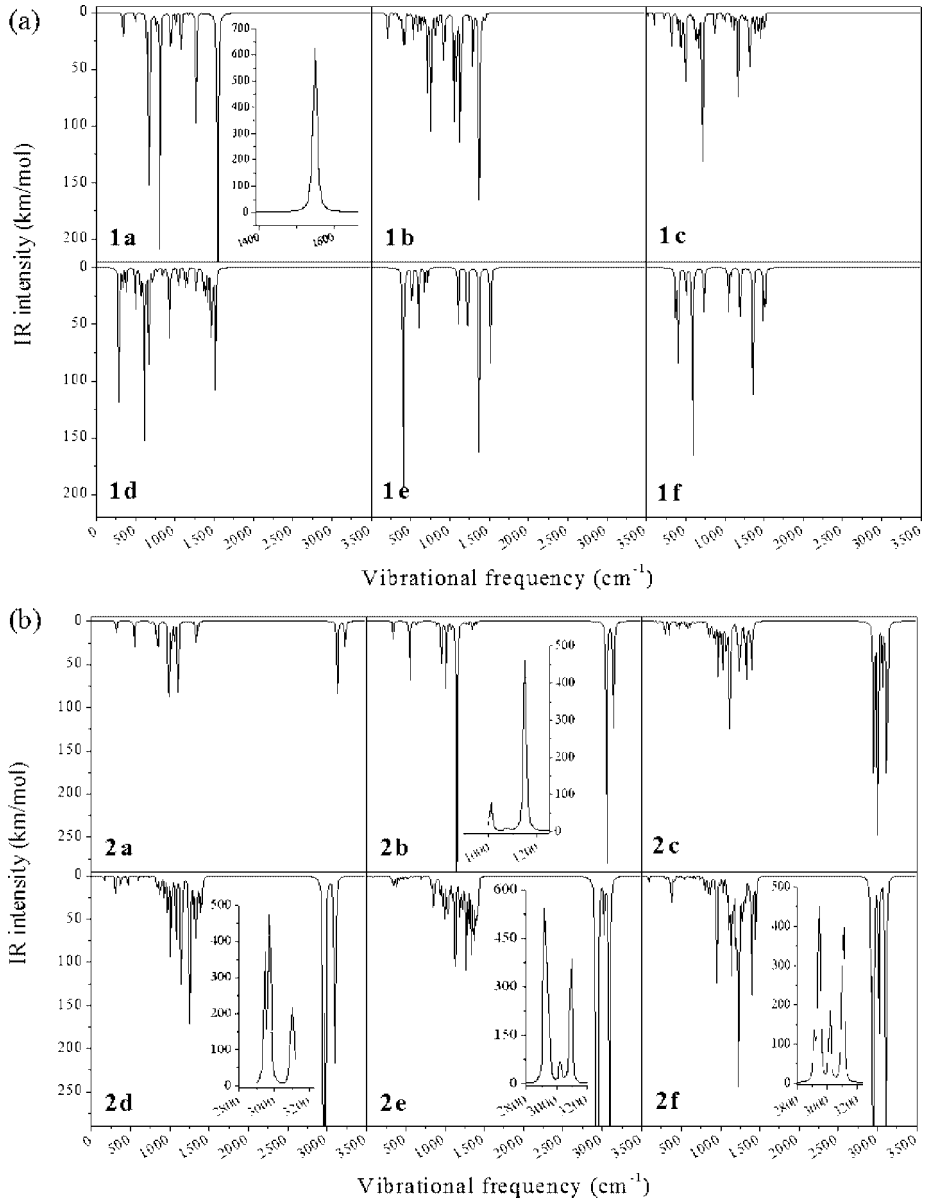

Figure 4. Simulated IR spectra of drum-like compounds $C_{4n}N_{2n}$ ($n = 3-8$) (a) and $C_{4n}H_{4n}N_n$ ($n = 3-8$) (b).

in Figure 3, the corresponding C−C bond lengths in cycloalkane, C_nH_{2n} ($n = 3-8$), were calculated at the B3LYP/6-31G** level. The calculated and averaged values of C−C bond lengths on the top or bottom polygon in $C_{4n}H_{4n}N_{2n}$ ($n = 3-8$) are 1.508, 1.558, 1.556, 1.560, 1.571, and 1.580 Å, respectively. And the corresponding C−C bond lengths in cycloalkane, C_nH_{2n} ($n = 3-8$) are 1.508, 1.557, 1.546, 1.537, 1.544, and 1.543 Å. It is found that the top or bottom polygon in $C_{4n}H_{4n}N_{2n}$ ($n = 3-8$) is kept planar, and the planar structure is also kept in cyclopropane and cyclobutane, but not in cycloalkane, C_nH_{2n} ($n = 5-8$). Therefore, the calculated values of C−C bond lengths in $C_{4n}H_{4n}N_{2n}$ ($n = 3, 4$) are consistent with those in cycloalkane, C_nH_{2n} ($n = 3, 4$), and there exists no such consistency of calculated C−C bond lengths between that in $C_{4n}H_{4n}N_{2n}$ ($n = 5-8$) and the corresponding one in cycloalkane, C_nH_{2n} ($n = 5-8$).

As for the abnormally short C−C bond lengths (1.508 Å) on the top or bottom polygon in **2a** compared with those (1.556−1.580 Å) of other $C_{4n}H_{4n}N_{2n}$ ($n = 4-8$) compounds, it will be justified by the strong σ conjugation effect in the triangle[42] revealed by the calculation of NICS in Section 3.5. As for the $C_{4n}N_{2n}$ ($n = 3-8$) series, the similar abnormality in the curve of the calculated value of C−C bond lengths on the top or bottom polygon in Figure 3 can also be partially explained for the same reason.

3.2. Vibrational Frequency and IR Spectrum Simulation. To verify whether the $C_{4n}N_{2n}$ ($n = 3-8$) and $C_{4n}H_{4n}N_{2n}$ ($n = 3-8$) molecules are at the minimum of the hypersurface of potential energy or not, vibrational frequencies have been calculated at the B3LYP/6-31G** level. Meanwhile, the simulated IR spectra will be useful for their future experimental identification.

The simulated IR spectra for $C_{4n}N_{2n}$ ($n = 3-8$) in the range of 0−3500 cm^{-1} and 0−220 km/mol intensity and for $C_{4n}H_{4n}N_{2n}$ ($n = 3-8$) in the range of 0−3500 cm^{-1} and 0−290 km/mol intensity are plotted in Figure 4. The strongest peak located at 1550 cm^{-1} for **1a** is assigned to a vibration mode corresponding to the alternative expand-shrink movement of the top and bottom C−C triangles.

The peak near 3000 cm^{-1} attributing to the C−H vibration frequency in the IR spectra for all hydrogenated compounds can be found in Figure 4(b). Actually, only the carbon atoms adjacent to nitrogen atoms, not all carbon atoms, are involved in these C−H

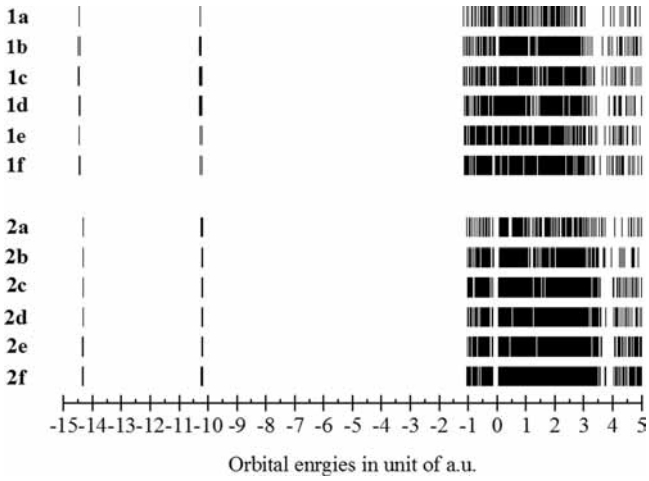

Figure 5. The orbital energy spectrum in $C_{4n}N_{2n}$ ($n = 3-8$) and $C_{4n}H_{4n}N_{2n}$ ($n = 3-8$) species (in au)

TABLE 2: The IP(eV), EA(eV), and Molecular Orbital Gap (ΔE, eV)

species	IP	EA	ΔE
1a	6.18	4.22	1.96
1b	6.04	4.35	1.69
1c	5.50	3.37	2.12
1d	5.22	3.32	1.90
1e	5.28	2.50	2.78
1f	5.39	2.39	2.99
2a	4.57	−1.66	6.23
2b	4.03	−1.31	5.33
2c	4.14	−1.14	5.28
2d	4.35	−0.98	5.33
2e	4.35	−1.01	5.36
2f	4.24	−0.98	5.22

vibrations. The intensity of the peak near 3000 cm^{-1} for **2d**, **2e**, and **2f** compounds is stronger than that for **2a**, **2b**, and **2c**.

3.3. Heat of Formation, Hydrogenation Reaction, and Stability. A systematic study on chemical stability for drum-like $C_{4n}N_{2n}$ ($n = 3-8$) and $C_{4n}H_{4n}N_{2n}$ ($n = 3-8$) compounds at the ground state is conducted by thermochemical calculation. Isodesmic reaction is one of the computational methods for gas-phase heat of formation ($\Delta H°_f$). For drum-like $C_{4n}N_{2n}$ ($n = 3-8$) and $C_{4n}H_{4n}N_{2n}$ ($n = 3-8$) molecules, the designed isodesmic reaction equations are presented as follows:

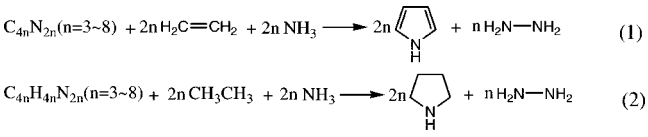

(1)

(2)

The experimental $\Delta H°_f$ of ethylene, ammonia, pyrrole, and hydrazine is used in eq 1, and the experimental $\Delta H°_f$ of ethane, ammonia, pyrrolidine, and hydrazine is used in eq 2. The calculated $\Delta H°_f$ is tabulated in Table 1. The detailed design of isodesmic reaction equations and those experimental values are provided in Supporting Information S2.

The concept of group energy and the group heat of formation (group $\Delta H°_f$)[43] are useful for discussion of the relative stability among $C_{4n}N_{2n}$ ($n = 3-8$) and $C_{4n}H_{4n}N_{2n}$ ($n = 3-8$) molecules. The group energies and group $\Delta H°_f$ were obtained from the calculated results of their total energies and $\Delta H°_f$. Their total energies and group energies of all these molecules with D_{nh} symmetry are provided in Supporting Information S3, which shows that the ascending order of group energy is $C_{32}N_{16}$ (D_{8h}) < $C_{28}N_{14}$ (D_{7h}) < $C_{24}N_{12}$ (D_{6h}) < $C_{20}N_{10}$ (D_{5h}) < $C_{16}N_8$ (D_{4h}) < $C_{12}N_6$ (D_{3h}). $C_{32}N_{16}$ (D_{8h}) and $C_{28}N_{14}$ (D_{7h}) are the more stable molecules. As for the $C_{4n}H_{4n}N_{2n}$ ($n = 3-8$) series in D_{nh}, $C_{12}H_{12}N_6$ (D_{3h}) is more stable than $C_{28}H_{28}N_{14}$ (D_{7h}) and $C_{32}H_{32}N_{16}$ (D_{8h}). $C_{16}H_{16}N_8$ (D_{4h}) is more stable than $C_{24}H_{24}N_{12}$ (D_{6h}), $C_{28}H_{28}N_{14}$ (D_{7h}), and $C_{32}H_{32}N_{16}$ (D_{8h}).

For the final optimized structures, **1a**, **1b**, **1c**, **1d**, **1e**, **1f**, **2a**, **2b**, **2c**, **2d**, **2e**, and **2f**, their group energies and group $\Delta H°_f$ are listed in Table 1. In $C_{4n}N_{2n}$ ($n = 3-8$) species, a descending order for group energies and group $\Delta H°_f$, **1a** > **1b** > **1c** > **1d** > **1e** > **1f**, is found. So the order of the relative stability of these molecules is **1f** > **1e** > **1d** > **1c** > **1b** > **1a**. The lowest group energy and group $\Delta H°_f$ for the case of **1f**(D_{8h}) indicates that it is the most stable molecule among $C_{4n}N_{2n}$ ($n = 3-8$) species. Also the **1f**(D_{8h}) is the molecule with the highest heat of formation, 1062.20 kcal/mol. So this molecule can be taken as an HEDM for future research. Compared with N_{24},[43] it is predictable that $C_{32}N_{16}$ could be synthesized easily in consideration of their comparable $\Delta H°_f$ values.

The hydrogenation of fullerenes is a basic reaction used to modify fullerenes chemically.[39] The hydrogenation of $C_{4n}N_{2n}$ ($n = 3-8$) species should also give the precursor

$$C_{4n}N_{2n} + 2nH_2 \rightarrow C_{4n}H_{4n}N_{2n}\ (n = 3-8) \qquad (3)$$

which can be modified subsequently, such as nitration etc. The negative ΔG of the hydrogenation reaction shown in Table 1 indicates that the hydrogenated drum-like $C_{4n}H_{4n}N_{2n}$ ($n = 3-8$) is more stable than $C_{4n}N_{2n}$ ($n = 3-8$). Table 1 also shows that the lowest ΔH and ΔG of the hydrogenation reaction are evolved for the case of **1b**, but not for the case of **1a**. **2c** has the lowest group energy and group $\Delta H°_f$. The five-membered ring is responsible for enhancing thermal stability of this molecule. The product of the nitration of $C_{20}H_{20}N_{10}$ might be a potential HEDM.

3.4. Orbital Energy. The attempt to explore the orbital energy of drum-like $C_{4n}N_{2n}$ ($n = 3-8$) and $C_{4n}H_{4n}N_{2n}$ ($n = 3-8$) species helps us to examine their electronic stability. As shown in Figure 5, the orbital energy distribution exhibits an increasing trend of continuity along with the increase of n ($n = 3-8$). The orbital gaps (LUMO-HOMO) near zero value are found to be larger for $C_{4n}H_{4n}N_{2n}$ ($n = 3-8$) than those of $C_{4n}N_{2n}$ ($n = 3-8$) apparently. This also indicates that $C_{4n}H_{4n}N_{2n}$ ($n =$

TABLE 3: NICS (ppm) for Drum-like $C_{4n}N_{2n}$ ($n = 3-8$) and $C_{4n}H_{4n}N_{2n}$ ($n = 3-8$) Cages[a]

species	NICS(**T**)	NICS(**C**)	NICS(**B**)	species	NICS(**C**)	NICS(**T**)	NICS(**B**)
1a	−31.78	−34.51	−31.78	**2a**	−43.66	4.70	−43.66
1b	−23.80	−14.63	−23.80	**2b**	−0.79	4.24	−0.79
1c	−14.77	−14.53	−14.77	**2c**	−4.23	1.17	−4.23
1d	−0.97	3.66	−0.97	**2d**	−3.35	1.71	−3.12
1e	−0.37	−6.35	−0.37	**2e**	0.50	2.43	0.50
1f	−1.91	−10.32	−1.91	**2f**	−0.84	0.85	−0.84

[a] **C**, **T**, and **B** denote the central points of the whole molecule and the ring centers of top and bottom polygons, respectively.

3−8) species are recognized as being more stable than $C_{4n}N_{2n}$ ($n = 3-8$) species. The orbital gap ΔE, IP(ionization potential), and EA(electron affinity) are also listed in Table 2.

In $C_{4n}N_{2n}$ ($n = 3-8$) species, **1f** shows the highest electronic stability because of the largest orbital gap. Due to lower orbital gap and higher EA for $C_{4n}N_{2n}$ ($n = 3-8$) species, it is more difficult to lose an electron but easier to accept one. Therefore, the hydrogenation reaction of **1f** gives the highest ΔG and **1b** gives the lowest ΔG. In $C_{4n}H_{4n}N_{2n}$ ($n = 3-8$) species, **2a** has the highest electronic stability. But for the $C_{4n}H_{4n}N_{2n}$ ($n = 3-8$) species with high energy gap and low EA, they turn out to have stable drum-like cages.

3.5. Aromatic Character. As known, electron delocalization may lead to hyperconjugation interaction, accordingly enhancing thermal stabilities of molecules. Aromatic character is an important index to characterize the electron delocalization. The aromatic character of a molecule at the specified position can be evaluated by the NICS value by using a ghost atom placed in this position. In this paper, NICS at three specified positions is investigated, i.e. the geometric center of molecule and the ring centers of top and bottom polygons. The calculated NICS values are listed in Table 3.

The negative NICS for a specified position means strong shielding effect, and thus high electron density existed thereabout. It is clear that there are six small positive NICS values in the cage centers of the $C_{4n}H_{4n}N_{2n}$ ($n = 3-8$) species, which indicates that there is weak antiaromatic character at these points. In the ring centers of top and bottom polygons of $C_{4n}H_{4n}N_{2n}$ ($n = 3-8$), **2a** shows the most negative or the lowest NICS value of −43.66, and **2b** shows an NICS value of −0.79. In comparison, the NICS value at the center of the triangle of cyclopropane is −42.57, and that for cyclobutane is 3.96 calculated at the same level. Similar dependence also exists in the C−C bond length of the polygon, i.e. the calculated value of this C−C bond length in **2a**'s triangle (1.508 Å) is the same as that in cyclopropane, and that in **2b**'s quadrangle (1.558 Å) is comparable to that in cyclobutane (1.557 Å). The almost zero NICS values existing in the two quadrangle centers in the top and bottom sites of **2b** represent zero aromatic character. **2e** and **2f** also show zero aromatic character at the center of the top and bottom polygons.

In $C_{4n}N_{2n}$ ($n = 3-8$) species, NICS values in the top and bottom polygon centers increase from $n = 3$ to 8 almost monotonically. It is noticed that the NICS values in the molecular center of the **1d** molecule are the highest among those at the same position in the $C_{4n}N_{2n}$ ($n = 3-8$) species. A strong delocalization effect over the lateral pyrrole rings might be indicated by the positive or almost zero NICS values at all three points of **1d**. The **1e** and **1f** molecules show a lower NICS value at their molecular center as compared with those at the centers of top and bottom rings.

As for the abnormality of **1a** in Figure 3, i.e. short bond lengths of both the C−C (1.409 Å) and N−N (1.351 Å) bonds, it can be explained by the very low NICS values at all three specified points (Table 3) due to the σ-conjugative effect in triangles and the Π-delocalization effect. Similarly, the strong σ-conjugative effect is also responsible for the short C−C bond length in **2a**. The abnormal NICS value of **2a** is caused by σ aromatic contribution at its top and bottom triangle centers.[42,44]

In the case of $C_{4n}N_{2n}$ ($n = 3-8$), there are several Π-delocalization orbitals formed, and thus there exists a high shielding effect in general. However, in the case of $C_{4n}H_{4n}N_{2n}$ ($n = 3-8$), there is no such Π-delocalization orbital, and thus no shielding effect except for the local σ-conjugative effect.

4. Conclusions

In the current work, 12 drum-like $C_{4n}N_{2n}$ ($n = 3-8$) and $C_{4n}H_{4n}N_{2n}$ ($n = 3-8$) cages were investigated by DFT theory. All geometries were optimized in local minima on the potential energy supersurface. Molecular structures, thermochemical properties, vibrational analysis, orbital energy, and NICS calculation were studied for the ground state. Our study focused on the relationship between molecular structures and the relative stabilities. Meanwhile, to find energy-containing molecules from those drum-like polynitrogen cages is another aim. The following conclusions are drawn:

(1) The $C_{4n}N_{2n}$ ($n = 3-8$) series exhibits a condensed structure due to the conjugation and cage effects, while the $C_{4n}H_{4n}N_{2n}$ ($n = 3-8$) series behaves quite normally. Except the abnormal structure for **1a** and **2a**, the increase of the N−N bond length accompanies the decrease of the C−C bond length from $n = 4$ to 8 in $C_{4n}N_{2n}$; in contrast the slight decrease of the N−N bond length accompanies the slight increase of the C−C bond length from $n = 4$ to 8 in $C_{4n}H_{4n}N_{2n}$.

(2) The calculation of the ΔG and ΔH of the hydrogenation of $C_{4n}N_{2n}$ ($n = 3-8$) shows that the reactions belong to the exothermic reaction at 298 K and the $C_{4n}H_{4n}N_{2n}$ ($n = 3-8$) is more stable than $C_{4n}N_{2n}$ ($n = 3-8$). Some of them are predicted to be stable and of high energy. Among $C_{4n}N_{2n}$ ($n = 3-8$), $C_{32}N_{16}$ is the most stable molecule with a very high gas-phase heat of formation of 1062.20 kcal/mol.

(3) The analysis of orbital energies and molecular aromatic character provides another insight about relative stability. Molecular relative stability for bigger cage-shaped molecules depends on not only their aromatic character but also the cage effect.

Supporting Information Available: Summary of the geometric parameters, related isodesmic reactions as well as the total energy and group energy of the $C_{4n}N_{2n}$ ($n = 3-8$) and $C_{4n}H_{4n}N_{2n}$ ($n = 3-8$) molecules with D_{nh} symmetry in detail. This material is available free of charge via the Internet at http://pubs.acs.org.

References and Notes

(1) Christe, K. O.; Wilson, W. W.; Sheehy, J. A.; Boatz, J. A. *Angew. Chem., Int. Ed.* **1999**, *38*, 2004.
(2) Vij, A.; Wilson, W. W.; Vij, V.; Tham, F. S.; Sheehy, J. A.; Christe, K. O. *J. Am. Chem. Soc.* **2001**, *123*, 6308.
(3) Vij, A.; Pavlovich, J. G.; Wilson, W. W.; Vij, V.; Christe, K. O. *Angew. Chem., Int. Ed.* **2002**, *41*, 3051.
(4) Butler, R. N.; Stephens, J. C.; Burke, L. A. *Chem. Commun.* **2003**, *8*, 1016.
(5) Glukhovtsev, M. N.; Jiao, H.; Schleyer, P. v. R. *Inorg. Chem.* **1996**, *35*, 7124.
(6) Leininger, M. L.; Van Huis, T. J.; Schaefer, H. F., III *J. Phys. Chem. A* **1997**, *101*, 4460.
(7) Fau, S.; Wilson, K. J.; Bartlett, R. J. *J. Phys. Chem. A* **2002**, *106*, 4639.
(8) Gagliardi, L.; Evangelisti, S.; Barone, V.; Roos, B. O. *Chem. Phys. Lett.* **2000**, *320*, 518.
(9) Li, Q.-S.; Hu, X.-G.; Xu, W.-G. *Chem. Phys. Lett.* **1998**, *287*, 94.
(10) Engelke, R.; Stine, J. R. *J. Phys. Chem.* **1990**, *94*, 5689.
(11) Schmidt, M. W.; Gordon, M. S.; Boatz, J. A. *Int. J. Quantum Chem.* **2000**, *76*, 434.
(12) Strout, D. L. *J. Phys. Chem. A* **2002**, *106*, 816.
(13) Bruney, L. Y.; Bledson, T. M.; Strout, D. L. *Inorg. Chem.* **2003**, *42*, 8117.
(14) Sturdivant, S. E.; Nelson, F. A.; Strout, D. L. *J. Phys. Chem. A* **2004**, *108*, 7087.
(15) Bliznyuk, A. A.; Shen, M; Schaefer, H. F., III *Chem. Phys. Lett.* **1992**, *198*, 249.
(16) Ha, T.-K.; Suleimenov, O.; Nguyen, M. T. *Chem. Phys. Lett.* **1999**, *315*, 327.
(17) Strout, D. L. *J. Phys. Chem. A* **2004**, *108*, 2555.

(18) Lein, M.; Frunzke, J.; Timoshkin, A.; Frenking, G. *Chem. Eur. J.* **2001**, *7*, 4155.
(19) Gagliardi, L.; Pyykkö, P. *J. Am. Chem. Soc.* **2001**, *123*, 9700.
(20) Burke, L. A.; Butler, R. N.; Stephens, J. C. *J. Chem. Soc., Perkin Trans. 2* **2001**, *9*, 1679.
(21) Straka, M.; Pyykkö, P. *Inorg. Chem.* **2003**, *42*, 8241.
(22) Wang, L. J.; Zgierski, M. Z.; Mezey, P. G. *J. Phys. Chem. A* **2003**, *107*, 2080.
(23) Cheng, L. P.; Li, Q. S. *J. Phys. Chem. A* **2004**, *108*, 665.
(24) Bruney, L. Y.; Strout, D. L. *J. Phys. Chem. A* **2003**, *107*, 5840.
(25) Strout, D. L. *J. Phys. Chem. A* **2003**, *107*, 1647.
(26) Wang, L.; Mezey, P. G. *J. Phys. Chem. A* **2005**, *109*, 3241.
(27) Jursic, B. S. *J. Mol. Struct. (THEOCHEM)* **2000**, *530*, 21.
(28) Zhou, G.; Pu, X.-M.; Wong, N.-B.; Tian, A.; Zhou, H. *J. Phys. Chem. A* **2006**, *110*, 4107.
(29) Disch, R. L.; Schulman, J. M. *J. Am. Chem. Soc.* **1988**, *110*, 2102.
(30) Ternansky, R. J.; Balogh, D. W.; Paquette, L. A. *J. Am. Chem. Soc.* **1982**, *104*, 4503.
(31) Attalla, M. I.; Vassallo, A. M.; Tattam, B. N.; Hanna, J. V. *J. Phys. Chem.* **1993**, *97*, 6329.
(32) Balasubramanian, K. *J. Phys. Chem.* **1993**, *97*, 4647.
(33) Wu, H.-S.; Qin, X.-F.; Xu, X.-H.; Jiao, H.; Schleyer, P. v. R. *J. Am. Chem. Soc.* **2005**, *127*, 2334.
(34) Chen, Z.; Jiao, H.; Hirsch, A.; Thiel, W. *Chem. Phys. Lett.* **2000**, *329*, 47.
(35) Chernichenko, K. Y.; Sumerin, V. V.; Shpanchenko, R. V.; Balenkova, E. S.; Nenajdenko, V. G. *Angew. Chem., Int. Ed.* **2006**, *45*, 7367.
(36) Paulus, B. *Phys. Chem. Chem. Phys.* **2003**, *5*, 3364.
(37) Malolepsza, E.; Witek, H. A.; Irle, S. *J. Phys. Chem. A* **2007**, *111*, 6649.
(38) Wu, H.-S.; Xu, X.-H.; Jiao, H.-J. *J. Phys. Chem. A* **2004**, *108*, 3813.
(39) Okamoto, Y. *J. Phys. Chem. A* **2001**, *105*, 7634.
(40) Strout, D. L. *J. Chem. Theory Comput.* **2005**, *1*, 561.
(41) Schleyer, P. v. R.; Maerker, C.; Dransfeld, A.; Jiao, H.; van Eikema Hommes, N. J. R. *J. Am. Chem. Soc.* **1996**, *118*, 6317.
(42) Moran, D.; Manoharan, M.; Heine, T.; Schleyer, P. v. R. *Org. Lett.* **2003**, *5*, 23.
(43) Zhou, H.; Wong, N.-B.; Zhou, G.; Tian, A. *J. Phys. Chem. A* **2006**, *110*, 3845.
(44) Fowler, P. W.; Baker, J.; Lillington, M. *Theor. Chem. Acc.* **2007**, *118*, 123.

JP801501G